

The role of mass transfer in solution photocatalysis at a supported titanium dioxide surface

Samina Ahmed, Claire E. Jones, Terence J. Kemp* and Patrick R. Unwin*

Department of Chemistry, University of Warwick, Coventry, UK CV4 7AL

Received 23rd August 1999, Accepted 8th October 1999

The kinetics of Cl^- production from the UV-photocatalysed degradation of aqueous 4-chlorophenol (CP), by a thin TiO_2 (Degussa P25) film, in both aerated and oxygenated solutions, have been determined by the channel flow method with electrochemical detection. The experimental approach allows surface kinetics and mass transport effects to be readily resolved. For typical irradiation intensities of $(0.7\text{--}2.0) \times 10^{17}$ quanta $\text{cm}^{-2} \text{s}^{-1}$, the results obtained with dilute CP solutions (≤ 0.5 mM), in particular, clearly demonstrate that there is a range of practically important conditions where mass transport plays a role in controlling the kinetics of the process. When these effects are considered, the surface kinetics are consistent with the Langmuir–Hinshelwood model.

Introduction

The application of UV-irradiated semiconductors, particularly TiO_2 , to the mineralisation of a very wide range of toxic organic species in aqueous solution, has been the subject of hundreds of articles and many reviews over the last few years.¹ The semiconductor is applied either as a colloidal slurry² or as a thin film^{3d} deposited on glass surfaces (beads, helices, tubes, plates). In the latter case, mass transport effects may play a significant role in controlling the overall rate, as evident from the flow-rate-dependent apparent rate constants that have been reported from previous studies in flow-through reactors.³

In order to better understand photodegradation kinetics in immobilised photocatalyst systems, it is recognised that the influence of both mass transfer and chemical kinetics must be taken into account.⁴ To this end, the degradation rate of 4-chlorophenol (CP) was recently investigated in a stirred reactor under conditions where mass transport was considered to be sufficiently high to have a negligible effect on the rate.⁵ This approach provides a potentially simple route for investigating the kinetics of photocatalysis, although experience from other areas suggests that such methods must be carefully applied and mass transport fully characterised.⁶ Surprisingly, apart from this one study,⁵ there are no other quantitative reports on the role of mass transport in controlling photodegradation rates.

Following our earlier application of a Ag/AgCl ultramicroelectrode⁷ to monitor Cl^- formation potentiometrically during the photomineralisation of 2,4-dichlorophenol at a TiO_2 film, we report a kinetic study of the TiO_2 film (Degussa P25)—sensitised photodegradation of CP in aerated and oxygenated solutions using the channel flow method with electrochemical detection (CFMED) as a new approach to identify the role of mass transfer in controlling the kinetics. It has been shown in other areas that CFMED provides both controlled and well-defined mass transport conditions, allowing interfacial kinetics to be readily identified.^{8–10} We describe here how the technique can be adapted to facilitate the quantitative study of photomineralisation kinetics, under conditions where contributions from surface and mass transport processes can be resolved.

Experimental

A home-built channel flow cell (Fig. 1) was employed that consisted of: (i) a PVC plate with inlet and outlet ports for solution flow, and a quartz window; (ii) an epoxy resin coverplate containing two Ag band electrodes that were 0.25 mm in length (measured along the cell) and 4.0 mm wide (across the cell), positioned upstream and downstream of a glass slide (12.0 mm long and 10.0 mm wide) onto which the TiO_2 film was deposited; (iii) a Teflon spacer (Goodfellow, Cambridge, UK), which produced a rectangular duct 45 mm long, 12 mm wide and 0.5 mm high, when the cell was assembled. A similar cell for the investigation of (dark) solid/liquid interfaces has been described more fully elsewhere.¹¹ The indicator electrode was positioned 2.0 mm from the downstream edge of the TiO_2 film, while the reference electrode was 8.0 mm from the upstream edge. As shown in Fig. 1, when the cell was assembled, the electrodes were in the shadow of the PVC

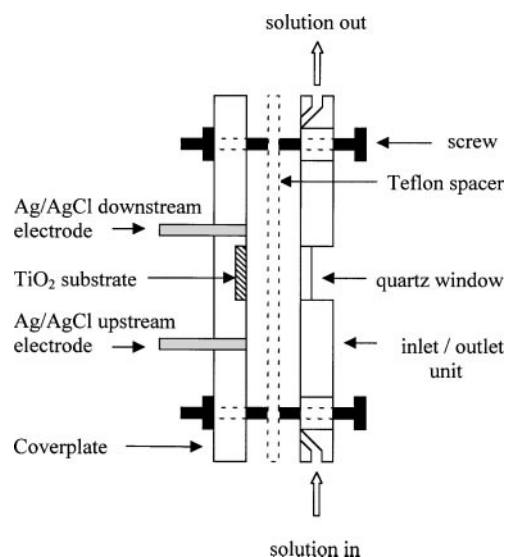


Fig. 1 Cross section of the channel flow cell used to investigate the TiO_2 -sensitised photodegradation of 4-chlorophenol.

plate, ensuring that there was no illumination of the electrode surfaces.

Before use, the coverplate was polished with a series of diamond lapping compounds (25–1 μm ; Kemet, UK), followed by 0.05 μm alumina (Buehler, USA). The Ag band electrodes were coated in AgCl and calibrated against standard KCl solutions as described elsewhere.⁷

An aqueous CP (Aldrich, purity 99%) solution (concentration in the range $(0.2\text{--}0.5) \times 10^{-3} \text{ mol dm}^{-3}$) was flowed through the cell from a reservoir using gravimetric feed, taking care to avoid any bubble formation in the system. For experiments under 1 atm† O_2 , the solution in the reservoir was purged with O_2 (99.5%, BOC) and the flow tubing (1.5 mm id, Omnifit) was jacketed with PVC tubing (12 mm id) through which oxygen was also passed.

A high powered xenon lamp (Illuminator 6000, Eurosep Instruments, Cergy-Pontoise, France) was used as the source of UV-irradiation. The intensity of the lamp was determined following a modification of the method developed by Hatchard and Parker,¹² and a full emittance profile has been determined.^{12b} The potential difference between the two Ag/AgCl electrodes was recorded on a Keithley 175 autoranging multimeter, as a function of flow rate, in the range $10^{-4}\text{--}10^{-1} \text{ cm}^3 \text{ s}^{-1}$. The photodegradation kinetics were monitored *via* the formation of Cl^- , determined by recording the potential difference between the downstream (indicator) and upstream (reference) electrodes. Although the in-flowing solution did not contain Cl^- , the upstream electrode maintained a constant reference potential, over all of the flow rates investigated, presumably due to the rapid dissolution kinetics of AgCl, ensuring that the upstream electrode was always in contact with a locally saturated solution of the sparingly soluble salt.¹³ Similar results were obtained when a saturated calomel electrode was employed as the reference electrode in the reservoir of the flow system. When the lamp was switched off, no detectable levels of Cl^- were produced by the flow of aqueous CP over the TiO_2 film.

The TiO_2 film was prepared from a Degussa P25 suspension,¹⁴ where 5 g of TiO_2 was mixed with 100 cm^3 Milli-Q (Millipore Corp.) reagent grade water (resistivity 18 $\text{M}\Omega \text{ cm}$), sonicated for 1 h and stirred for 5 h with a magnetic stirrer. The suspension was dropped onto the glass surface of the coverplate and then dried with Ar gas. This process was typically repeated five times, to achieve an even, complete coating. The coverplate was dried in an oven at 373 K for 12 h, resulting in a mechanically stable film. The topography of the film was imaged under water using a Digital Instruments (Santa Barbara, California, USA) Nanoscope-E atomic force microscope (AFM), equipped with a standard fluid cell, operating in contact mode.

Results and discussion

Typical height and deflection mode images of a small area of the TiO_2 -film surface are shown in Fig. 2. Both images show that the preparation method results in a fairly compact film. The distances between some of the boundaries defining the particles are consistent with the mean particle size of 30 nm,¹ while apparent larger separations suggest the agglomeration of several particles. The small height variations in Fig. 2(a) indicate that the film is fairly smooth on the scale of channel flow measurements. The degree of surface roughness is similar to that of a polished electrode and so is not expected to disrupt solution flow through the channel.

Fig. 3 shows the potential difference between the indicator and reference electrodes, as a function of flow rate, for an

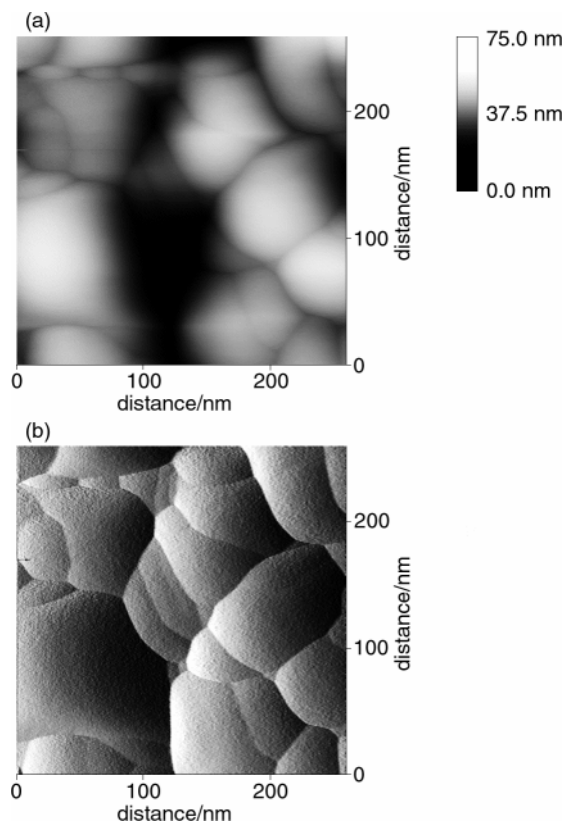


Fig. 2 AFM images of the topography of the TiO_2 film: (a) height mode image and (b) deflection mode image.

aerated solution containing $5.0 \times 10^{-4} \text{ mol dm}^{-3}$ CP in a flow cell with and without a TiO_2 film, with irradiation through the quartz window at an intensity of $2.0 \times 10^{17} \text{ quanta cm}^{-2} \text{ s}^{-1}$. In the absence of TiO_2 , there is no detectable potential difference between the two electrodes, over the entire range of flow rates studied, indicating that Cl^- is not produced from aqueous CP by direct irradiation of the zone between the indicator and reference electrodes. In contrast, at the same irradiation intensity, with TiO_2 present, a sizeable potential difference is established, which increases as the flow rate decreases (attaining values up to 30 mV). This behaviour can be attributed to the formation of Cl^- at the TiO_2 surface, due to the photodegradation of CP, with Cl^- subsequently detected at the downstream electrode. The reaction occurs

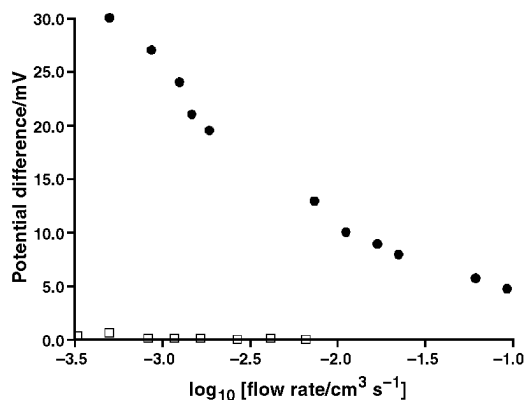
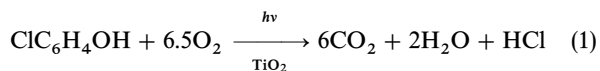


Fig. 3 Potential difference between the indicator and reference electrodes, as a function of log (flow rate), for an aerated solution containing $5.0 \times 10^{-4} \text{ mol dm}^{-3}$ 4-chlorophenol with (●) and without (□) a TiO_2 film. UV illumination intensity was $2.0 \times 10^{17} \text{ quanta cm}^{-2} \text{ s}^{-1}$.

† 1 atm = 101 325 Pa.

with the following stoichiometry:⁵



In a colloidal TiO_2 slurry, the kinetics follow the Langmuir-Hinshelwood model¹

$$\text{rate} = \frac{\gamma K_{\text{O}_2} [\text{O}_2] I_a^m K_{\text{CP}} [\text{CP}]}{(1 + K_{\text{O}_2} [\text{O}_2])(1 + K_{\text{CP}} [\text{CP}])} \quad (2)$$

where K_{O_2} and K_{CP} are the equilibrium adsorption constants for O_2 and CP, respectively, at the TiO_2 surface, I_a is the light flux, m is a power term (varying between 0.5 and 1.0), and γ is a proportionality constant.

This rate law has also been considered to apply to immobilised catalysts, but for all studies considered, it has been assumed that the concentration of CP at the catalyst surface remains the same as that in the bulk solution, which is inappropriate if mass transport of CP becomes a significant parameter in controlling the rate.

The kinetics of the photomineralisation process were analysed considering two limits. At the simplest level, we considered the case where there is no depletion of either O_2 or CP at the TiO_2 surface. In this case, for a given light intensity and bulk concentrations of CP and O_2 , all terms in eqn. (2) are constant and we may write for this surface-limited model:

$$\text{rate} = k'_{\text{SL}} \quad (3)$$

If the transport of CP onto the TiO_2 surface is considered to be significant (without any change of the interfacial concentration of O_2 from that in the bulk solution), the rate law for this mixed-control model can be written as:

$$\text{rate} = k'_{\text{MC}} \frac{K_{\text{CP}} [\text{CP}]_s}{(1 + K_{\text{CP}} [\text{CP}]_s)} \quad (4)$$

where the subscript 's' indicates the surface concentration.

The well-defined mass transport of the channel flow cell⁸ enables us to calculate the local concentrations of Cl^- at the detector electrode as a function of flow rate, geometry and kinetics for each of the two candidate rate laws. With reference to the coordinate system in Fig. 4, the transport of Cl^- (in both the surface-limited and mixed-control models) and CP (in the mixed-control model only), under steady-state conditions, is governed by:

$$D_{\text{CP}} \frac{\partial^2 [\text{CP}]}{\partial y^2} = v_0 \left[1 - \frac{(y-h)^2}{h^2} \right] \frac{\partial [\text{CP}]}{\partial x} \quad (5)$$

$$D_{\text{Cl}^-} \frac{\partial^2 [\text{Cl}^-]}{\partial y^2} = v_0 \left[1 - \frac{(y-h)^2}{h^2} \right] \frac{\partial [\text{Cl}^-]}{\partial x} \quad (6)$$

The x and y coordinates are defined in Fig. 4. D_i denotes the diffusion coefficient of species i (Cl^- or CP) and v_0 is the fluid velocity in the centre of the channel. This latter variable is related to the volume flow rate, V_f , and geometry of the channel by:

$$v_0 = \frac{3V_f}{4hd} \quad (7)$$

where h is the channel half-height and d is the channel width.

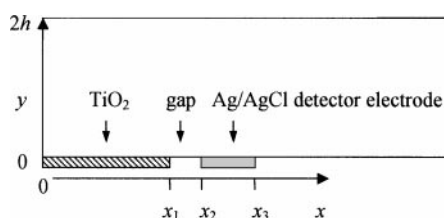


Fig. 4 Coordinate system for CFMED simulations.

The two rate laws embodied in eqn. (3) and (4) form the boundary conditions at the TiO_2 surface:

$y = 0, 0 \leq x < x_1$:

$$D_{\text{CP}} \frac{\partial [\text{CP}]}{\partial y} = -D_{\text{Cl}^-} \frac{\partial [\text{Cl}^-]}{\partial y} = k'_{\text{SL}} \quad (8)$$

$$D_{\text{CP}} \frac{\partial [\text{CP}]}{\partial y} = -D_{\text{Cl}^-} \frac{\partial [\text{Cl}^-]}{\partial y} = k'_{\text{MC}} \frac{K_{\text{CP}} [\text{CP}]_{y=0}}{1 + K_{\text{CP}} [\text{CP}]_{y=0}} \quad (9)$$

The value for D_{CP} was calculated as $0.94 \times 10^{-5} \text{ cm}^2 \text{ s}^{-1}$ using the Wilke-Chang equation,¹⁵ while the literature values^{3d,16} for $D_{\text{Cl}^-} = 1.9 \times 10^{-5} \text{ cm}^2 \text{ s}^{-1}$ and $K_{\text{CP}} = 4.9 \times 10^3 \text{ M}^{-1}$ were used. Values for K_{CP} up to $3 \times 10^4 \text{ M}^{-1}$ have been reported for studies in suspensions,¹⁷ but this value did not provide a good description of our experimental results; the lower value employed is appropriate to thin-film systems.^{3d} The effective diffusion coefficient of Cl^- will depend on the counter cation, which is unknown under the conditions of our experiments. However, simulations showed that the value of D_{Cl^-} , when varied over the maximum possible range of 1.5×10^{-5} – $3.5 \times 10^{-5} \text{ cm}^2 \text{ s}^{-1}$, had only a minor effect on the calculated detector electrode response, under the defined experimental conditions.

Additional boundary conditions for the other walls of the channel are:

$y = 0, x_1 < x \leq x_3$:

$$D_{\text{CP}} \frac{\partial [\text{CP}]}{\partial y} = D_{\text{Cl}^-} \frac{\partial [\text{Cl}^-]}{\partial y} = 0 \quad (10)$$

$y = 2h, \text{ all } x$:

$$D_{\text{CP}} \frac{\partial [\text{CP}]}{\partial y} = D_{\text{Cl}^-} \frac{\partial [\text{Cl}^-]}{\partial y} = 0 \quad (11)$$

and $x < 0, \text{ all } y$:

$$\begin{aligned} [\text{Cl}^-] &= 0 \\ [\text{CP}] &= [\text{CP}]^* \end{aligned} \quad (12)$$

where the asterisk superscript represents the bulk concentration.

The problem outlined above was readily solved using the backwards implicit finite difference method, which has been applied extensively to steady-state CFMED problems.⁸ For a given cell geometry and flow rate, the simulation provided values for $[\text{Cl}^-]$ at the downstream electrode, for the two models, which could then be compared to the experimental data.

We first consider the analysis of the data shown in Fig. 3. After converting the potential difference response to $[\text{Cl}^-]$ at the downstream electrode, the data shown in Fig. 5 were obtained. The data are shown alongside the best fits for the two models, which clearly indicates that the mixed-control model, embodied by eqn. (4), provides the optimum description, especially in that it predicts the experimentally observed tendency of $[\text{Cl}^-]$ to level off towards $[\text{CP}]^*$, at low flow rate. For this experimental data a value of $k'_{\text{MC}} = 4.1 \times 10^{-10} \text{ mol cm}^2 \text{ s}^{-1}$ was found to be the most appropriate.

The importance of mass transport effects was highlighted by Turchi and Ollis, specifically for dilute solutions.⁴ Accordingly, we next consider the photodegradation kinetics of CP at $2.0 \times 10^{-4} \text{ mol dm}^{-3}$ bulk concentration in solutions that were either aerated or oxygenated with 1 atm O_2 (Fig. 6). For these studies the light intensity was reduced to $7.0 \times 10^{16} \text{ quanta cm}^{-2} \text{ s}^{-1}$. In both cases, the experimental results conform more closely to the mixed-control model, rather than the surface-limited model, with $k'_{\text{MC}} = 1.5 \times 10^{-10} \text{ mol cm}^{-2} \text{ s}^{-1}$ (aerated solution) and $k'_{\text{MC}} = 4.5 \times 10^{-10} \text{ mol cm}^{-2} \text{ s}^{-1}$ (oxygenated solution). These data underline the importance of

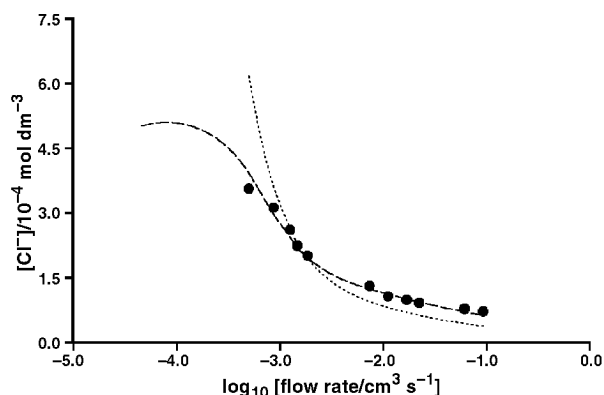


Fig. 5 $[\text{Cl}^-]$ at the downstream detector electrode (●) as a function of \log (flow rate) for $5.0 \times 10^{-4} \text{ mol dm}^{-3}$ 4-chlorophenol solution (aerated). The best fits are shown for the mixed-controlled model (dashed line, with $k'_{\text{MC}} = 4.1 \times 10^{-10} \text{ mol cm}^{-2} \text{ s}^{-1}$) and the surface-limited model (dotted line with $k'_{\text{SL}} = 1.5 \times 10^{-10} \text{ mol cm}^{-2} \text{ s}^{-1}$).

mass transport in controlling the rate of photomineralisation at lower substrate concentrations. Comparison of the analysed data in Fig. 5 and 6(a) suggests that under aerated solution conditions, the apparent rate constant is closely proportional to the light intensity and the exponent, m , in eqn. (2) is effectively unity. Similar behaviour was found in the stirred reactor studies of Mills and Wang.⁵ The presence of higher levels of O_2 speeds up the surface photomineralisation process (Fig. 6(b)) and the role of mass transport becomes clearer over the whole range of flow rates considered.

It is useful to identify when mass transport will be important generally compared to the surface kinetics of the photomineralisation process. For a given light intensity and oxygen

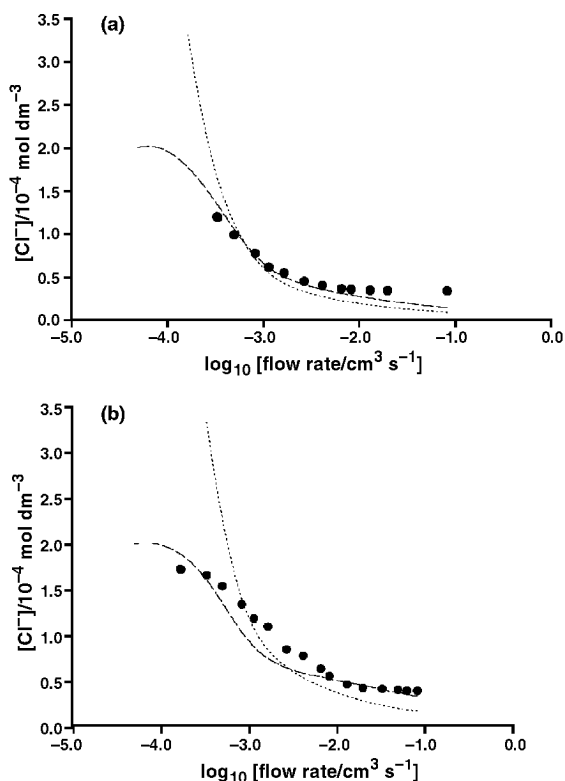


Fig. 6 $[\text{Cl}^-]$ at the downstream detector electrode (●) as a function of \log (flow rate) for $2.0 \times 10^{-4} \text{ mol dm}^{-3}$ 4-chlorophenol solution, for both aerated (a) and oxygenated (b) solution conditions. In each case, the best fits are shown for the mixed control model (dashed lines, simulated with $k'_{\text{MC}} = 1.5 \times 10^{-10} \text{ mol cm}^{-2} \text{ s}^{-1}$ (a) and $k'_{\text{MC}} = 4.5 \times 10^{-10}$ (b)) and the surface limited model (dotted lines, simulated with $k'_{\text{SL}} = 0.4 \times 10^{-10} \text{ mol cm}^{-2} \text{ s}^{-1}$ (a) and $k'_{\text{SL}} = 0.4 \times 10^{-10} \text{ mol cm}^{-2} \text{ s}^{-1}$ (b)), the light intensity was $7.0 \times 10^{16} \text{ quanta cm}^{-2} \text{ s}^{-1}$.

level (assuming depletion effects are negligible), the key parameters are the mass transfer coefficient, k_t , and the bulk concentration of CP. For dilute CP solutions, where $K_{\text{CP}}[\text{CP}] \ll 1$, we may conclude from the present studies that mass transport will be important when $k_t < k'_{\text{MC}}K_{\text{CP}}$. Under the conditions of the experiments in this paper, the latter product has a value in the range 7×10^{-4} – $2.2 \times 10^{-3} \text{ cm s}^{-1}$.

Finally, it is informative to estimate the quantum yield of the photomineralisation process. The quantum yield is flow-rate dependent, attaining a maximum value when mass transport is sufficiently high to be unimportant. In the high flow rate limit, the data in Fig. 5 and 6(a) correspond to quantum yields of 8.8×10^{-4} and 6.4×10^{-4} , respectively. Increasing the level of oxygen in solution increases the quantum yield to *ca.* 1.9×10^{-3} .

Conclusions

CFMED represents a powerful new approach for quantitatively investigating heterogeneous photomineralisation kinetics. The initial studies reported in this paper show that, for dilute (sub-millimolar) solutions, mass transport is a key parameter in controlling the photomineralisation rate of CP. Further studies, employing this methodology to examine a wider range of reaction conditions and compare the kinetics for different chlorophenols are now underway. It is also likely that there will be conditions where O_2 transport to the catalyst surface will play a role in the kinetics of the process. These possible effects are also under investigation with CFMED.

Acknowledgements

We thank the Ministry of Science and Technology, Government of Bangladesh, for a scholarship for SA.

References

- See for example: (a) A. Mills and S. Le Hunte, *J. Photochem. Photobiol. A: Chem.*, 1997, **108**, 1; (b) A. Mills, R. H. Davies and D. Worsley, *Chem. Soc. Rev.*, 1993, **22**, 417; (c) A. L. Linsebigler, G. Lu and J. T. Yates, Jr., *Chem Rev.*, 1995, **95**, 735.
- (a) J. Cunningham and P. Sedlak, *J. Photochem. Photobiol. A: Chem.*, 1994, **77**, 255; (b) M. Barbeni, E. Pramauro, E. Pelizzetti, E. Borgarello, M. Gratzel and N. Serpone, *Nouv. J. Chim.*, 1984, **8**, 547; (c) J.-C. D'Oliveira, G. Al-Sayyed and P. Pichat, *J. Environ. Sci. Technol.*, 1990, **24**, 990; (d) J.-C. D'Oliveira, C. Minero, E. Pelizzetti and P. Pichat, *J. Photochem. Photobiol. A: Chem.*, 1993, **72**, 261; (e) R. W. Matthews, *Water Res.*, 1986, **20**, 569; (f) R. W. Matthews, *Water Res.*, 1990, **24**(5), 653; (g) L. Rideh, A. Wahrer, D. Ronze and A. Zoulalian, *Ind. Engg. Chem. Res.*, 1997, **36**, 4712.
- (a) M. Bideau, B. Claudel, C. Dubien, L. Faure and H. Kazouan, *J. Photochem. Photobiol. A: Chem.*, 1995, **91**, 137; (b) K. Hofstadler, R. Bauer, S. Novalic and G. Heisler, *J. Environ. Sci. Technol.*, 1994, **28**, 670; (c) H. Al-Ekabi and N. Serpone, *J. Phys. Chem.*, 1988, **92**, 5726; (d) R. W. Matthews, *J. Catal.*, 1988, **111**, 264; (e) R. W. Matthews, *J. Phys. Chem.*, 1987, **91**, 3328; (f) K. Tennakone, C. T. K. Tilakaratne and I. R. M. Kottegoda, *J. Photochem. Photobiol. A: Chem.*, 1995, **87**, 177; (g) R. W. Matthews and S. R. McEvoy, *J. Photochem. Photobiol. A: Chem.*, 1992, **64**, 231; (h) A. Sclafani, A. Brucato and L. Rizzuti, *Photocatalytic Treatment of Water and Air*, ed. D. F. Ollis and H. Al-Ekabi, Elsevier, Amsterdam, 1993, 533.
- C. S. Turchi and D. F. Ollis, *J. Phys. Chem.*, 1988, **92**, 6852.
- A. Mills and J. Wang, *J. Photochem. Photobiol. A: Chem.*, 1998, **118**, 53.
- E. L. Sjöberg and D. Rickard, *Geochim. Cosmochim. Acta*, 1983, **47**, 2281.
- T. J. Kemp, P. R. Unwin and L. Vincze, *J. Chem. Soc., Faraday Trans.*, 1995, **91**(21), 3893.
- See for example: (a) P. R. Unwin, A. J. Barwise and R. G. Compton, *J. Colloid Interface Sci.*, 1989, **128**, 208; (b) R. G. Compton, K. L. Prichard and P. R. Unwin, *Chem. Commun.*, 1989, 249; (c) R. G. Compton and P. R. Unwin, *Philos. Trans. R.*

- Soc. London, Ser. A*, 1990, **330**, 1; (d) R. G. Compton and K. L. Prichard, *Philos. Trans. R. Soc. London, Ser. A, London*, 1990, **330**, 47; (e) C. A. Brown, R. G. Compton and C. A. Narramore, *J. Colloid Interface Sci.*, 1993, **160**, 1517; (f) R. G. Compton and C. A. Brown, *J. Colloid Interface Sci.*, 1994, **165**, 445.
- 9 (a) P. R. Unwin and J. V. Macpherson, *Chem. Soc. Rev.*, 1995, **24**, 109; (b) J. V. Macpherson and P. R. Unwin, *Prog. React. Kinet.*, 1995, **20**, 185; (c) P. R. Unwin, *J. Chem. Soc., Faraday Trans.*, 1998, **94**, 3183; (d) P. R. Unwin and R. G. Compton, *Compr. Chem. Kinet.*, 1989, **29**, 173.
- 10 For a review of photoelectrochemical applications of channel electrodes see: R. G. Compton and R. A. W. Dryfe, *Prog. React. Kinet.*, 1995, **20**, 245.
- 11 R. Orton and P. R. Unwin, *J. Chem. Soc., Faraday Trans.*, 1993, **89**, 3947.
- 12 (a) C. G. Hatchard and C. A. Parker, *Proc. R. Soc. London, Ser. A*, 1956, **235**, 518; (b) L. Vincze, T. J. Kemp and P. R. Unwin, *J. Photochem. Photobiol. A: Chem.*, 1999, **123**, 7.
- 13 J. V. Macpherson and P. R. Unwin, *J. Phys. Chem.*, 1995, **99**, 14824.
- 14 A. Mills, D. Worsley and R. H. Davies, *J. Chem. Soc., Chem. Commun.*, 1994, 2677.
- 15 C. R. Wilke and P. Chang, *AIChE J.*, 1955, **1**(2), 264.
- 16 J. S. Newman, *Electrochemical Systems*, Prentice Hall, Englewood Cliffs, NJ, 1991.
- 17 A. Mills and S. Morris, *J. Photochem. Photobiol. A: Chem.*, 1993, **70**, 183.

Paper 9/06819H